REFINEMENT OF THE CRYSTAL STRUCTURE OF A NATURAL GEHLENITE, $Ca_2Al(Al,Si)_2O_7$

S. JOHN LOUISNATHAN *

Department of Geological Sciences
Virginia Polytechnic Institute and State University, Blacksburg, Virginia, 24061

Abstract

The crystal structure of gehlenite, $Ca_2Al(Al,Si)_2O_7$, was refined to $R' = 3.7\%$ from 3D diffractometer data. Silicon and aluminum show partial ordering with Al in tetrahedra at point $\bar{4}$, and $Al_{1/2}Si_{1/2}$ in tetrahedra at point symmetry *m*. Cross-hatched and lamellar structures observed in gehlenite, from Crestmore, California, are interpreted as twinning. Certain genetic aspects of such twinning are considered in terms of Al,Si ordering.

Introduction

The crystal structure of a synthetic gehlenite was determined by Raaz (1930) and that of an intermediate melilite by Warren (1930). Though their work established the general features of the crystal structure, the nature of Al, Si, and Mg distribution among the tetrahedral sites could not be inferred. Smith (1953), on reexamining the structure of a natural melilite, was able to propose certain ordering schemes. He pointed out the importance of refining the crystal structures of both synthetic and natural gehlenite for understanding the order-disorder phenomena in melilites. Korczak & Raaz (1967) refined the structures of a synthetic gehlenite and a synthetic gallium-gehlenite, $Ca_2Ga(Ga,Si)_2O_7$. They found partial ordering: $Al_{1.0}$ or $Ga_{1.0}$ in the $\bar{4}$ tetrahedral sites and $Al_{0.5}Si_{0.5}$ or $Ga_{0.5}Si_{0.5}$ in the tetrahedral sites of point symmetry *m*. Sahama & Lehtinen (1967) obtained infrared evidence of the same Al, Si distribution in a natural gehlenite.

Experimental

The specimen chosen was from the contact metamorphic limestone complex of Crestmore, California. Chemical analysis, undertaken by the author, utilized the *x*-ray emission microanalysis technique. Averaging

* Previous address: Department of Geophysical Sciences, The University of Chicago, Chicago, Illinois.

TABLE 1. COMPARISON BETWEEN THE POWDER PATTERN OBTAINED USING MANY GRAINS AND A SINGLE GRAIN OF CRESTMORE GEHLENITE

hkl	I^c/I_1^c	Diffractometer Pattern with Cu/Ni Rad.			Photographic Pattern with Fe/Mn Rad.		
		I^p/I_1^p	d_{obs}	d_{cal}	I	d_{obs}	d_{cal}
110	—	5	5.449	5.457	w	5.457	5.459
001	5	5	5.081	5.087	w	5.081	5.085
101	5	9	4.231	4.247	w	4.243	4.246
111	31	28	3.711	3.721	s	3.722	3.721
210	8	2	3.475	3.451	vw	3.450	3.452
201	43	27	3.066	3.074	s	3.074	3.074
211	100	100	2.848	2.856	vs	2.857	2.856
220	32	15	2.738	2.729	m	2.730	2.729
002	26	15	2.547	2.543	m	2.535	2.542
310	38	32	2.437	2.441	m-s	2.441	2.441
102	20	12	2.421	2.415	m	2.415	2.415
221	30	30	2.408	2.405	s	2.406	2.405
112	9	4	2.314	2.305	vw	2.305	2.305
301	31	19	2.291	2.296	m	2.299	2.296
311	3	3	2.206	2.200	vw	2.199	2.201
202	3	4	2.117	2.125	—	—	—
122	14	10	2.038	2.047	m	2.048	2.047
321	6	4	1.970	1.973	—	—	—
400	64	55	1.921	1.929	vs	1.930	1.930
410	17	8	1.876	1.872	w	1.872	1.872
222	8	4	1.865	1.860	vw	1.860	1.860
330	75	55	1.818	1.819	s	1.819	1.820
302	2	7	1.812	1.809	w	1.809	1.809
312	36	45	1.768	1.761	s	1.7608	1.7609
411	12	8	1.753	1.757	w	1.7568	1.7570
420	28	8	1.723	1.726	m	1.7264	1.7261
113	4	10	1.612	1.619	m	1.6190	1.6189
521	31	25	1.376	1.379	s	1.3790	1.3797
				$a_{cal} = 7.716$ $c_{cal} = 5.089$		$a_{cal} = 7.720$ $c_{cal} = 5.085$	

$$\frac{I^c}{I_1^c} = \frac{\text{Single crystal, } I\ (hkl) \times p(hkl)}{\text{Single crystal, } I\ (211) \times p(211)} \times 100\,.\ (p = \text{multiplicity})$$

$$\frac{I^p}{I_1^p} = \frac{\text{Powder data peak height of } (hkl)}{\text{Powder data peak height of } (211)} \times 100$$

the results obtained on three different grains and correcting the data according to the procedure of Smith (1965), yielded the following formula when calculated on the basis of seven oxygen atoms :

$$(Ca_{1.96}Sr_{0.03}Mn_{0.01})\ [Al_{1.93}Mg_{0.05}Fe_{0.02}Si_{1.02}]\ O_7.$$

Counts for Na were nearly zero. The standards used were anorthite glass (CP 11) and Mt. Anakie feldspar (CP 8) for Ca, Na, Al, Si, and Sr; and a clinopyroxene (CS 10) for Si, Mg, Fe, and Mn. Two of the analyzed grains showed irregular undulatory extinction under the polarizing microscope, but all three grains were homogeneous within 1 per cent and were of the same composition.

A diffractometer powder pattern of gehlenite with spectrographically pure silicon as the internal standard was obtained using Ni-filtered CuK_α radiation. The 2θ values, read to $\pm$ 0.01°, were corrected using the known positions of the silicon lines, and the cell dimensions were calculated and refined by the least squares method. The refinement was not satisfactory. The differences in $|d_{obs}-d_{cal}|$ and the errors in the refined cell dimensions were large. Compositional variation as a source of such errors was excluded since the microprobe analysis showed no such variation. In a later section, it will be suggested that the gehlenite grains from Crestmore show varying deviations from orthogonal geometry

TABLE 2. CELL-DIMENSIONS OF CRESTMORE GEHLENITE

Edge	Dimension in Å	Error in Å	Method
a	7.716	0.008	Cu/Ni Diffractometer pattern using many grains.
c	5.089	0.009	3 cycles of LS refinement with all reflections.
a	7.709	0.004	Cu/Ni Diffractometer pattern using many grains.
c	5.092	0.005	3 cycles of LS refinement with lines of $I > I^c/I_1^c = 20$.
a	7.706	0.005	Cu/Ni Diffractometer pattern using many grains.
c	5.069	0.007	3 cycles of LS refinement using only the last 14 high angle lines of Table 1. col. 4.
a	7.7195	0.0016	Fe/Mn Photographic pattern of a single grain.
c	5.0853	0.0017	3 cycles of LS refinement with all reflections.
a	7.7173*	0.0006	Fe/Mn Photographic pattern of a single grain.
c	5.0860*	0.0008	3 cycles of LS refinement with lines of $I > I^c/I_1^c = 20$.

* These values were used in the LS refinement of the crystal structure and in the calculation of interatomic distances and bond angles.

due to varying degrees of Al, Si ordering. It is believed that the unusually large residuals in the refinement of the cell edges come from such a variation in cell parameters. A single grain of gehlenite free from optical anomalies was ground with silicon as the internal standard and a powder pattern was made with a 114.6 mm camera using Mn-filtered FeK_α radiation. The refinement of the cell dimensions from these data was satisfactory. Table 1 compares the powder data obtained using the single grain (photographic pattern) with those obtained from using many grains of gehlenite (diffractometer pattern). In Table 2 are given the cell dimensions as obtained from both these sets of data.

Several thin sections of the rock containing gehlenite, from Crestmore, were studied. The rock consists essentially of gehlenite and merwinite; the accessory minerals in the decreasing order of abundance are: clinopyroxene, plagioclase, spurrite, garnet, vesuvianite, and calcite. Varying degrees of the following optical anomalies were observed in almost all the gehlenite grains: anomalous birefringence on (001), irregular undulatory extinction, extinction suggesting that the grains were made up of aggregates of parallel fibers, roughly square-shaped patches of extinction on (001) or on planes nearly parallel to (001), and $2V$ varying from nearly zero to 15°. The anomalous birefringence on (001), measured by Berek compensator on grains oriented on a universal stage, varied from 0.0003 to 0.0018. The error of measurement by this method is normally $\pm$ 2 per cent, however, in the case of the present study, the error is estimated to approximate 20 per cent since orientation of the grains was difficult due to the optical anomalies described above. A few grains showed lamellae, observed more readily in sections parallel or nearby to (001). Some of these are shown in Figures 1 and 2: Figure 1a shows broad lamellae with one composition plane well defined and two not so well defined; Figure 1b shows fine polysynthetic lamellae with three broad lamella at right angles; Figure 2 a,b shows a cross-hatched polysynthetic intergrowth in gehlenite. Though the lamellae shown in these figures bear a remarkable resemblance to twin lamellae observed in K-feldspars, they are by no means so readily observed in gehlenite. Strong illumination and sometimes a tilt on the universal stage is required. Universal stage study indicates that the lamellar and the intergrowth structures could be polysynthetic twinning. This study also indicates that the optical anomalies described above may be due to domains of very fine polysynthetic twinning. Optical orientation of the grains shown in Figures 1 and 2 revealed the composition planes of the lamellae to be parallel to the c-axis. When the c-axis is parallel to the microscope axis, the angle between the two sets of crosshatched lamellae is 90°.

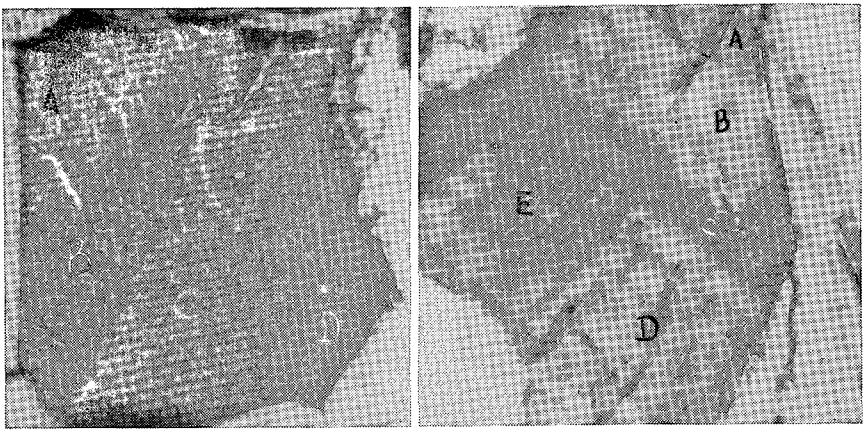

FIG. 1. Lamellar structure in gehlenite. (a, left) The greyish grain marked by ABCD is a gehlenite from the gehlenite-merwinite rock of Crestmore, California. The composition plane between B and C is more well defined than between A and B or C and D. Magnification 155 ×. (b) A grain of gehlenite from the same locality showing four broad lamellae A, B, C, and D. In the region E, very fine polysynthetic lamellae are observed. Magnification 155 ×.

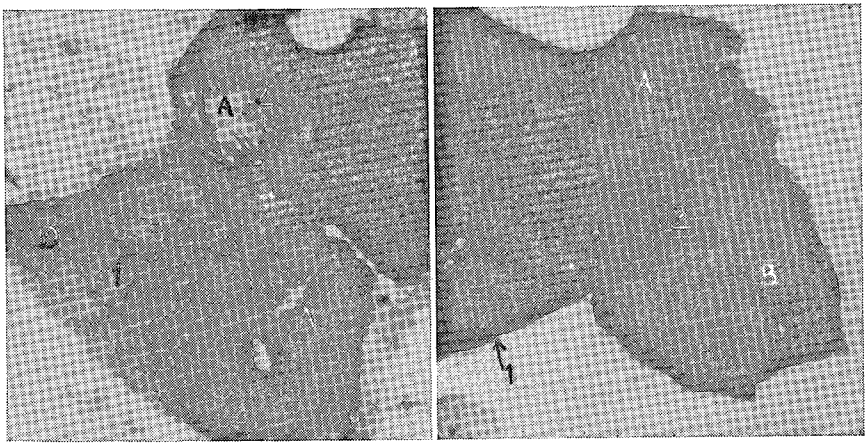

FIG. 2. Cross-hatched structure in gehlenite. (a, left) The grains marked 1 and 2 are gehlenite from Crestmore, California. Both the grains show cross-hatched lamellar structure. In grain 1, the region around A show intense cross-hatching, while in the region around D practically no cross-hatching is observed. The birefringence along c axis in region A of grain 1 is 0.0014 and 0.0003 in region D. Magnification 155 ×. (b) Cross-hatched lamellae in gehlenite; grain 2 of this figure is the grain 2 of (a) above in another orientation. In region A, very fine lamellar structure, and in region B cross-hatched structure are observed. The birefringence along c axis is 0.0018 in region A and 0.0012 in region B. Magnification 155 ×.

Optical study of a few thin sections made from rock chips that had been heated to *ca.* 800° C. for 3 to 8 days showed that all of the aforementioned anomalies had disappeared except for a consistent non-zero $2V$. In addition, a general decrease in the birefringence was noticed. The anomalous birefringence on (001) was of the order of 0.0004 with several grains showing "ultra-blue" interference color at the extinction position. Thin sections of a gehlenite-bearing rock from Trentino, Italy, kindly lent by Dr. Olsen of the Chicago Natural History Museum, do not show any twinning or any significant departure from perfect extinction; however, all gehlenite grains show a uniform $2V$ of about 4°.

Precession photographs of a gehlenite grain with cross-hatched structure are shown in Figure 3a,b. In Figure 3a, the precession axis is the crystallographic a-axis. In Figure 3b, the precession axis is the crystallographic [110] direction. Both photographs were made from the same single crystal. In Figure 3a, multiple spots are associated with (040), (001), (021), and (031) reflections. Diffuse streaks of varying intensities are associated with a few other ($0kl$) reflections. Figure 3b does not show any multiple spots. An explanation for this can be given as follows. The true unit cell of this gehlenite is triclinic, with (001) $\wedge$ (110) nearer to 90° than (001) $\wedge$ (100); in certain domains of the single

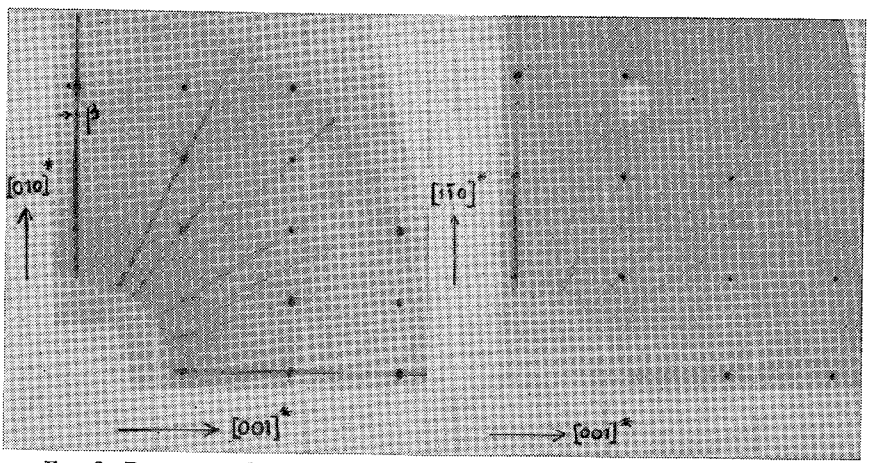

FIG. 3. Precession photographs of gehlenite that showed cross-hatched structure. One quadrant of the precession photograph of a gehlenite grain from Crestmore, California, that showed cross-hatched structure. CuK_α radiation was used. In (a) the precession axis is crystallographic a-axis. Multiple spots are associated with (040), (001), (002), (021), and (031) Bragg maxima. In (b) the precession axis is the (110) direction. This photograph of the same crystal does not show any multiple spots. The photographs also show some CuK_β spots, one such spot is indicated on the photograph.

crystal, the triclinic cells are polysynthetically twinned on {110} and {1$\bar{1}$0}. The triclinicity and the twin laws thus deduced could be accepted only with some reservations. The resolution of the split-spots are very poor for some reflections and strain effects could not be completely ruled out as a cause of spot-splitting. Several *x*-ray photographs of grains with not-so-well defined composition planes were also made. Such photographs show diffuse streaks associated with many Bragg maxima. One such photograph is shown in Figure 4. An *x*-ray photograph of a gehlenite grain selected from a heated (*ca.* 800° C. for 6 days) rock also showed streaks associated with many strong reflections. In analogy with a similar phenomenon occurring in orthoclase, the diffuse streaks from gehlenite crystals can be explained as due to domains of submicroscopic twinning. Again, strain effects as the cause of the optical and *x*-ray anomalies cannot be completely ruled out. If the observed lamellar structures are accepted as twin-lamellae, then a genetic explanation of their origin in terms of Al-Si ordering can be given. This is considered in detail in another section of this chapter.

A tabular grain of gehlenite, from Crestmore, of nearly 0.004 mm^3 volume, which did not show either spot-splitting or streaks of observable

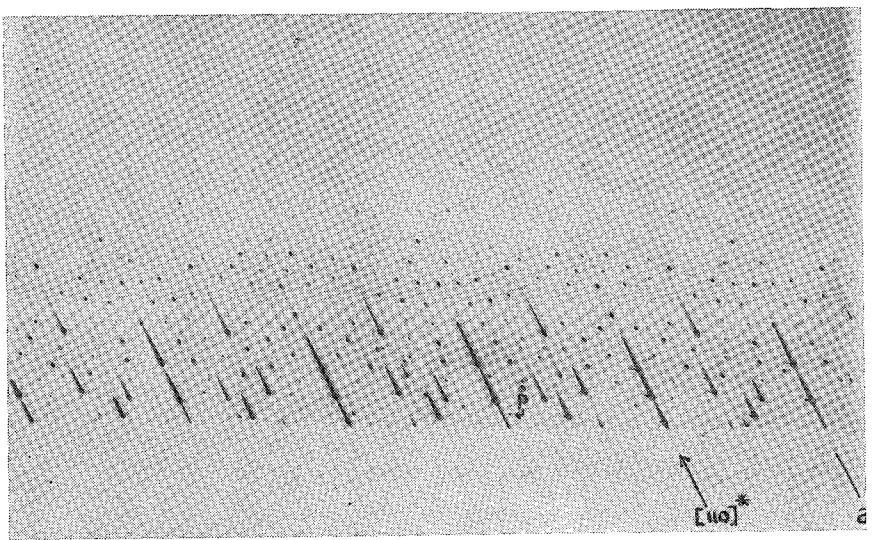

FIG. 4. Weissenberg photograph of gehlenite that showed diffuse lamellar structure. The grain was plucked out of a thin-section. Under the microscope this grain showed diffuse lamellar structure. Mo$K\alpha$ radiation was used. Diffuse streaks of varying intensities are associated with many (*hkl*) Bragg maxima. A tiny grain of pyroxene, which was sticking to the gehlenite grain, is the source for some spurious spots such as those marked "P" in the photograph.

intensity associated with the Bragg maxima, was chosen for structure analysis. The grain was mounted on the crystallographic b-axis. Precession and Weissenberg photographs showed no detectable deviation from tetragonal symmetry; the space group extinctions were carefully checked and found conformable to $P\bar{4}2_1m$. One thousand four hundred and eighty-seven intensities up to a limit of $\sin\theta/\lambda = 1.15$, representing the octants hkl, $\bar{h}k\bar{l}$, and $h\bar{k}\bar{l}$ were collected on a manual scintillation-counter-diffractometer of Weissenberg geometry, using Zr-filtered MoK_α radiation. The observed intensities were corrected for Lorentz, and polarization effects. The size and shape of the crystal was carefully measured and an absorption correction for polyhedral transmission was applied using the GNABS program of C. W. Burnam (private communication).

Refinement

The structural parameters were refined by the least squares technique using the SORFLS program (a local modified version of Busing, Martin & Levy 1962). The refinement began with the atomic coordinates given by Smith (1953) for an intermediate melilite, yielding an initial $R = 0.30$.

The melilite structure, in space group $P\bar{4}2_1m$, has two sets of non equivalent tetrahedral sites $T_{1,2}$ and $T_{3\text{-}6}$ (see Figure 5a). Gehlenite may be either fully ordered with Si in the two equivalent tetrahedra T_1 and T_2, and Al in the four equivalent tetrahedra T_3–T_6; or, partially ordered with Al in T_1 and T_2, and $Si_{0.5}Al_{0.5}$ in T_3–T_6. Two sets of refinements, corresponding to the two schemes above, were made using the following weighting scheme :

$$w = \left[x + \left(\frac{y}{I-B} \right) \left(\frac{I+B}{I-B} \right) \right]^{-1}$$

where I is the number of counts obtained for the peak without the background, B the number of background counts with y taken as unity. In this weighting scheme, the quantity

$$\left[\left(\frac{y}{I-B} \right) \left(\frac{I+B}{I-B} \right) \right]^{\frac{1}{2}}$$

was considered an estimate of standard deviation, $\sigma_{I(hkl)}$, following a procedure similar to that described by Evans (1961). The scattering functions of Al^{2+} and Si^{2+} come very close to one another in the region

of sin θ/λ between 0.15 and 0.33 and again in the region where sin $\theta/\lambda > 1.03$. Taking $x = 2$ in the above weighting scheme for the reflections falling in these regions and $x = 1$ for the rest of the data, an attempt was made to distinguish between the two ordering schemes described above. After four cycles of refinement with isotropic temperature factors and individual scale factors for each k-layer, diffractometer-setting, the set with Al in T_1 and T_2, and $Al_{0.5}Si_{0.5}$ in T_3–T_6 gave a weighted R' of 0.156 and the other set with Si in T_1 and T_2, and Al in T_3–T_6 an $R' = 0.165$. A calculation of interatomic distances at this stage showed that T_1 and T_2 (mean T–O distance 1.77 ± 0.01Å) were indeed larger than T_3–T_6 (mean T–O distance 1.68 ± 0.01Å). Based on these results, further refinements with Si in T_1 were discontinued. The refinement with Al in T_1 and $Al_{0.5}Si_{0.5}$ in T_3 was continued until the R′ dropped to 0.10 when anomalous correction terms with $f'_{Ca}=0.20$, $f''_{Ca}=0.40$; $f'_{Si}=0.10$; $f''_{Si}=0.10$; and $f'_{Al}=0.10$, $f''_{Al}=0.10$ were introduced and the refinements continued. At a stage when $R'=0.090$, seven pairs of symmetry related reflections and four inferior individual reflections were removed, and anisotropic temperature factors were introduced. The refinement continued until R' dropped to 0.072. For further refinements, the following weighting scheme was employed :

$$w = \left[x \cdot \left(\frac{y}{I-B} \right) \cdot \left(\frac{I+B}{I-B} \right) \right]^{-1}$$

with x, I, and B as specified earlier and $y = F^2$. This weighting scheme and the one used before appeared justified for the gehlenite data, since the quantity $g = \{\Sigma[w(|F_{obs}-F_{cal}|)^2]/(NO-NV)\}^{1/2}$, (where NO is the number of observations and NV the number of parameters varied) was close to unity. For an ideal weighting scheme, this quantity should equal unity (see, e.g., Hamilton 1964). In order to determine the absolute configuration and thus minimize the polar dispersion errors in the interatomic distances, two sets of refinements, one with (hkl), $(\bar{h}\bar{k}\bar{l})$, and $(h\bar{k}l)$ and the other with these indices inverted were performed. After four cycles of refinement, the former set gave an $R'=0.0492$ and the latter $R'=0.0491$. The differences in the z-coordinates of oxygen atoms with respect to Ca of the order of 0.0005. Though the differences between the two polarities is not very obvious, Hamilton's (1964) significance tests show that the refinement on $(\bar{h}\bar{k}\bar{l})$, (hkl), and $(\bar{h}kl)$, that gives $R' = 0.0491$, could be preferred to the other at 90 percent confidence level. After three more cycles on this polarity, the refinement converged to $R'=0.038$. The unweighted R was 0.139 at this stage. Such a high dif-

ference between R and R' is attributed to the use of a very large number of very weak reflections whose $\sigma_{I(hkl)}$ were larger than or nearly of the order of the $F(hkl)$. Omitting reflections with $F(hkl)/F_{max}(hkl) < 0.06$ and $\sigma_{I(hkl)} > 10.0$, and with only 759 data the R was 0.087 and R' was 0.037. The final atomic coordinates, site occupancy indices, and the thermal vibration parameters of the atoms in gehlenite are given in Tables 3 and 4.

Interatomic distances and bond angles, together with the estimated standard deviations in these quantities, were calculated using the SORFFE program (a local modified version of the ORFFE written by Busing, Martin & Levy [1964]). Calculations of the e.s.d.'s in interatomic dis-

TABLE 3. ATOMIC COORDINATES AND SITE OCCUPANCY INDICES IN GEHLENITE

Atoms	x	y	z	Site occupancy index	
				Ideal	Observed
Ca	0.3375(01)	1/2-x	0.5110(02)	1/2	0.484(01)
$T_{1,2}$	0.0	0.0	0.0	1/4	0.239(01)
$T_{3,6}$	0.1431(01)	1/2-x	0.9528(03)	1/2	0.489(01)
O(1)	0.5	0.0	0.1884(09)	1/4	0.249(02)
O(2)	0.1418(03)	1/2-x	0.2832(05)	1/2	0.508(03)
O(3)	0.0872(02)	0.1706(03)	0.8033(04)	1	1.046(04)

Numbers in parentheses are the *e.s.d.* $\times 10^4$ for positional coordinates and $\times 10^3$ for site occupancy indices.
$T_{1,2} = Al$, $T_{3\text{-}6} = Al_{0.5}Si_{0.5}$

TABLE 4. THERMAL VIBRATION PARAMETERS OF GEHLENITE

Atoms	β_{11}	β_{22}	β_{33}	β_{12}	β_{13}	β_{23}
Ca	0.0057(01)	β_{11}	0.0243(05)	0.0015(01)	−0.0013(02)	$-\beta_{13}$
$T_{1,2}$	0.0028*	β_{11}	0.0168(7)	0.0	0.0	0.0
$T_{3\text{-}6}$	0.0027(01)	β_{11}	0.0137(05)	0.0006(02)	−0.0008(02)	$-\beta_{13}$
O(1)	0.0099(06)	β_{11}	0.0132(16)	0.0023(10)	0.0	0.0
O(2)	0.0061(03)	β_{11}	0.0211(16)	−0.0009(06)	−0.0005(07)	$-\beta_{13}$
O(3)	0.0075(04)	0.0056(03)	0.0215(09)	0.0021(03)	−0.0007(06)	−0.0024(05)

Since different scale factors were used for the k-layers, β_{11} and β_{22} of $T_{1,2}$ were not varied after converting isotropic temperature factors to anisotropic factors.

Numbers in parentheses are the e.s.d. $\times 10^4$.

tances and bond angles were done taking into account both the errors in the cell-dimensions and those in the structural parameters. The bond distances and bond angles in gehlenite, presented in Table 5, do not include any corrections for the thermal movements of the atoms.

Discussion

Interatomic distances in gehlenite

This study confirms the general features of the structure as determined by Raaz (1930) but offers more information on the nature of Al-Si ordering. The Al-O and Si-O tetrahedral distances vary depending on the extent of tetrahedral linkages and on the neighboring non-tetrahedral cations (Smith & Bailey 1963). In gehlenite, the tetrahedron T_1 is linked to four other tetrahedra (T_3, T_4, T_5, and T_6) and thus T_1 resembles

Table 5. Bond Lengths and Angles in Gehlenite

Bond lengths in Å		Bond angles in degrees	
The (AlO_4) tetrahedron at point symmetry $\bar{4}$			
4Al–O(3)	1.785(2)	2O(3)–Al–O(3′)	118.8(1)
2O(3)–O(3′)	2.958(4)	4O(3)–Al–O(3″)	108.3(1)
4O(3)–O(3″)	2.977(2)		
The (T_2O_7) group at point symmetry $mm2$; with $T = Al_{0.5}Si_{0.5}$			
T(3)–O(1)	1.718(6)	T(3)–O(1)–T(3′)	130.6(3)
T(3)–O(2)	1.681(1)	O(1)–T(3)–O(2)	114.2(1)
2T(3)–O(3)	1.683(3)	2O(1)–T(3)–O(3)	101.3(2)
O(1)–O(2)	2.854(6)	O(3)–T(3)–O(3‴)	103.5(3)
2O(1)–O(34)	2.630(2)	2O(3)–T(3)–O(2)	117.1(2)
2O(3)–O(2)	2.869(3)	Mean	109.08
O(3)–O(3′)	2.643(4)		
The (CaO_8) polyhedron at point symmetry m			
2Ca–O(3)	2.439(2)	2O(2)–Ca–O(3)	64.9(1)
Ca–O(2)	2.429(7)	O(3)–Ca–O(3′)	65.6(1)
Ca–O(1)	2.416(4)	O(2)–Ca–O(2″)	60.8(2)
2Ca–O(3‴′)	2.815(2)	2O(2)–Ca–O(3′)	89.9(1)
2Ca–O(2′)	2.576(5)	2O(2′)–Ca–O(3′)	82.5(1)
		2O(1)–Ca–O(3′)	61.8(3)
		O(1)–Ca–O(2‴)	108.8(1)
		O(3″)–Ca–O(3‴)	131.9(2)

Numbers in parentheses are the e.s.d. for bond lengths × 10^3, for bond angles × 10.

a tetrahedron in framework aluminosilicate structures. O(3) is bonded to T_1, to one T_3 cation, and to two Ca atoms. The T_1–O(3) distance of 1.785 ± 0.002Å in gehlenite compares well with the mean Al–O distance of 1.780 ± 0.004Å in anorthite, where the mean is taken over four Al–O distances in tetrahedra whose oxygen atoms have two neighboring Ca atoms. Smith & Bailey (1963) found that Al–O distances varied from 1.75Å in frameworks to 1.77Å in sheets. Hence, the distance of 1.785Å in gehlenite indicates that T_1 is pure AlO_4 tetrahedron.

The T_3 type tetrahedra in gehlenite resemble those in layered aluminosilicates. With T_1 occupied solely by Al, it is necessary in the melilite structure that $T_{3\text{-}6}$ have an occupancy of $Al_{0.5}Si_{0.5}$. The mean T_3–O distance of 1.691 ± 0.004Å in gehlenite is in good agreement with the $Al_{0.5}Si_{05.}$–O distance of 1.69Å read off the Smith-Bailey curve for Al, Si–O distances in sheet structures.

The variations in the individual T–O distances and the Ca–O distances are in accordance with the nature of chemical bonding in melilite structures as discussed in the description of the crystal structure of hardystonite Louisnathan (1969).

Space group and twinning in gehlenite

Figure 5a is a projection of the tetrahedral linkages in melilite. Keeping the general features of the structure unaltered, two configurations with singular tetrahedral occupancies are shown in Figure 5b1 and b2. Configurations with Si in $T_{1,2}$ are not discussed here since this work has clearly shown that these are solely occupied by Al. The structures in Figure 5b are necessarily ordered with respect to Al and Si, and an inspection of these figures reveals $P2$ space group symmetry for Figure 5 b1 and $P1$ for Figure 5b2. If the true space group of melilite is $P2$ or $P1$, but tetragonal with $a \simeq b \neq c$, and $\alpha \simeq \beta \simeq \gamma \simeq 90°$ within the errors of observation, then a least squares refinement of atomic positional parameters with anisotropic thermal vibrational factors and with the symmetry restrictions of $P\bar{4}2_1m$ space group will average the dimensions of the tetrahedra $T_{3\text{-}6}$.

The only direct observation of the triclinic nature of the unit cell of gehlenite has been pointed out earlier. It is proposed that the true space group of a fully ordered gehlenite is $P1$, pseudotetragonal. The observed cross-hatched and lamellar structures in the Crestmore gehlenite have been interpreted as twinning. Two schemes of polysynthetic twinning are shown in Figure 5c,d. In Figure 5c, the twinning axis is c, and with the composition plane $\{010\}$ or $\{100\}$, polysynthetic lamellar twin-

ning is obtained, or with composition planes both {010} and {100} polysynthetic cross-hatched twinning is obtained. In Figure 5d, the twinning axis is c, and with composition plane {110} polysynthetic lamellar twinning, or with composition planes both {110} and {1$\bar{1}$0} polysynthetic cross-hatched twinning is obtained. Twinning according to these laws distributes Si and Al in all the four tetrahedra $T_{3\text{-}6}$. In a very finely twinned crystal, such a distribution of Al and Si introduces

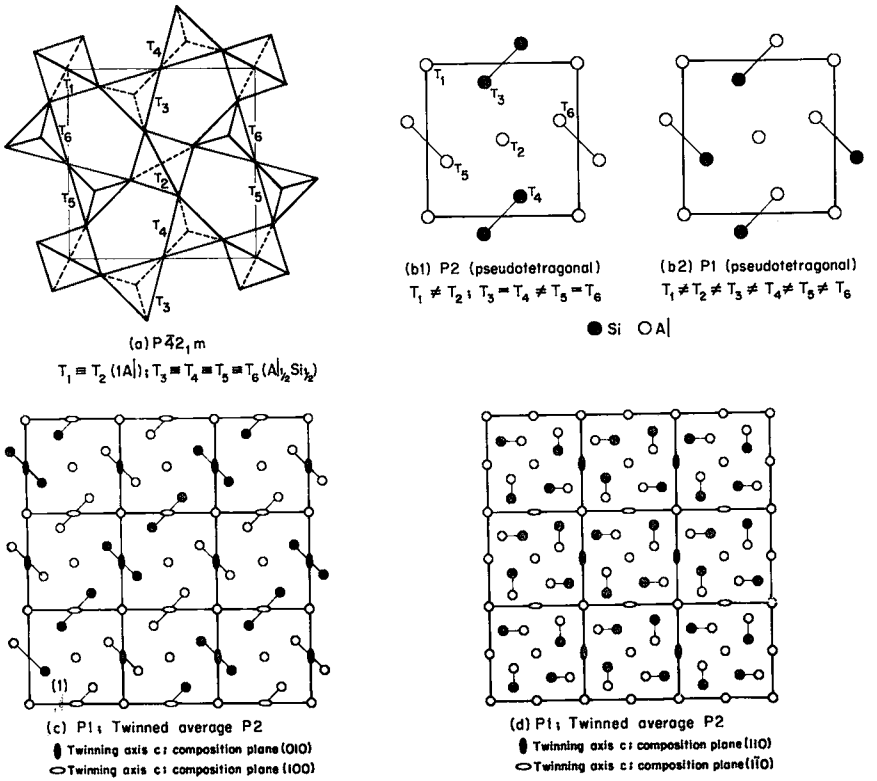

FIG. 5. Space group and twinning of gehlenite. (a) The tetrahedral linkages in the gehlenite structure, projected along c axis. (b1) and (b2) Two possible Al, Si distributions for a fully ordered gehlenite. (b1) corresponds to *P*2 and (b2) to *P*1 space groups. (c) A *c*-axis projection of nine adjacent unit cells of gehlenite obtained by twinning the *P*1 configuration on {100} and {010}. Twinning distributes Al and Si in all four tetrahedra, $T_{3\text{-}6}$. This leads to an average space group *P*2, pseudo $P\bar{4}2_1m$. In this *c*-axis projection, *a*-axis of gehlenite is taken along the *c*-face diagonal (along T_1–T_2–T_1). Nine adjacent unit cells of gehlenite obtained by twinning the *P*1 configuration on {110} and {1$\bar{1}$0} are shown. Twinning distributes Al and Si in all four tetrahedra, $T_{3\text{-}6}$. The leads to an average group *P*2, pseudo $C\bar{4}m2_1$.

a pseudo $\bar{4}$ symmetry along c[001]. Tetrahedral sites T_1 and T_2 are occupied by Al which introduces a pseudo 2_1 symmetry along a[100] and b[010]. Thus a finely twinned gehlenite assumes a pseudo $P\bar{4}2_1m$ space group symmetry.

The twinned structure with composition planes as $\{110\}$ and $\{1\bar{1}0\}$ should be slightly more stable than the one with twin-composition planes as $\{010\}$ or $\{100\}$, for in the latter there are several five-membered rings of AlO_4 tetrahedra while in the former there is at least one SiO_4 tetrahedron for every five-membered ring of tetrahedra. The twin laws exhibited by the two grains in Figure 6 appear to be $\{110\}$ and $\{1\bar{1}0\}$. However, experimental exidence is not wholly convincing to discard $\{100\}$ and $\{010\}$ twin laws for these grains. Deer, Howie & Zussman (1962) have reported that twin laws on $\{100\}$ and $\{010\}$ have also been found in some melilites.

In Figure 5c,d, the individual unit cells are fully ordered with respect to Al and Si. An important feature of the ordered gehlenite structure is that there are two oxygens in every Al-tetrahedra that are shared by another Al-tetrahedron. Synthetic $BaAl_2O_4$ (Perrotta & Smith 1968) also contains tetrahedral Al-O-Al linkages.

The tetrahedral dimensions indicating an occupancy of $Al_{0.5}Si_{0.5}$ for $T_{3\text{-}6}$ represent an average for two tetrahedra, one of pure Si and another of pure Al. The physical significance of such a fractional site occupancy can be explained by one or the other of the following two possibilities: (1) gehlenite, from Crestmore, crystallized statistically disordered in space group $P\bar{4}2_1m$, that is, Al and Si mixed over each of the tetrahedral sites $T_{3\text{-}6}$, (2) it crystallized fully ordered in space group $P1$, but polysynthetically twinned in such fine dimensions that the diffraction experiments could not reveal the order. Accordingly, the observed twinning may indicate either a tendency toward complete ordering of Al and Si from an initial low order or extension of ordered structure into larger domains.

The broad lamellae in Figure 1 a, b appear to suggest that those twin lamellae may be primary, that is, these are growth twins. The fine lamellae in region E of the grain in Figure 1 b appear as secondary twinning, that is, twinning associated with ordering process. Lack of sharp boundaries between the broad lamellae may suggest that these too may be secondary twinning. Thus the broader lamellae may represent extended regions of ordered domains.

The observed optical anomalies, as well as the diffuse streaks associated with the Bragg spectra, may now be given a satisfactory explanation as due to varying sizes and shapes of ordered domains. It was mentioned

earlier that the least squares refinement of the cell dimensions using the diffractometer data, which employed a number of grains, was generally unsatisfactory. A possible explanation for this is that various domains may have different degrees of ordering and as a result have slight differences in their cell dimensions.

Conclusion

The results of the present reinvestigation of the gehlenite crystal structure may be summarized as follows :

1. In the gehlenite end of the melilite series, there is at least partial ordering of Al and Si with $Al_{1.0}$ in $T_{1,2}$, and Al $_{0.5}Si_{0.5}$ in $T_{3\text{-}6}$.
2. Polysynthetic twinning, both lamellar and cross-hatched, may indicate a tendency toward complete ordering of Al and Si.
3. Twinning has been found in one specimen of gehlenite from a metamorphic rock. A gehlenite from a volcanic rock does not show twinning but does show a non-zero optic axial angle.
4. Strain effects cannot be ruled out.

Acknowledgments

I am grateful to Professors Joseph V. Smith and Paul B. Moore for their critical discussions and helpful suggestions during the entire course of this study. The financial support for this work came from NSF-GA 907 grant, administered to Dr. P. B. Moore.

References

Busing, W.R., Martin, K.O. & Levy, H.A. (1962) : ORFLS, A Fortran crystallographic least squares program. *Oak Ridge National Lab.*, Oak Ridge, Tennessee, U.S.A.

———— (1964) : ORFEE, A Fortran crystallographic functions and error program. *Oak Ridge National Lab.*, Oak Ridge, Tennessee, U.S.A.

Deer, W.A., Howie, R.A. & Zussman, J. (1962) : *Rock forming minerals*, vol. 1. Ortho- and ring-silicates, 236, London.

Evans, T. (1961) : Weighting factors for single crystal X-ray diffraction intensity data. *Acta Crystallogr.*, **14,** 689.

Hamilton, W.G. (1964) : *Statistics in physical science.* New York : The Ronald Press Company.

Korczak, P. & Raaz, F. (1967) : Verfeinerung der Kristallstruktur von Gehlenit unter Zugrundelegung des Gallium-Gehlenites. *Österreich. Akad. Wiss. Sitzung math.-natruwiss. K. Nr.*, **13,** 383-387.

Louisnathan, S.J. (1969) : The refinement of the crystal structure of hardystonite $Ca_2ZnSi_2O_7$. *Z. Kristallogr.*, **130,** 427-437.

Perrotta, A.J. & Smith, J.V. (1968) : The crystal structure of $BaAl_2O_4$. *Bull. Soc. franc. Min. Crist.*, **91,** 85-87.

RAAZ, F. (1930) : Die Struktur des synthetischen Gehlenit, $2CaO.Al_2O_3.SiO_2$. *Anzeiger Akad. Wiss. Wien. Math.-naturwiss. Kl. Nr.*, **18,** 203.

SAHAMA, Th.G. & LEHTINEN, M. (1967) : Infra-red absorption of melilite. *Compt. Rend. Soc. geologique Finlande,* **229,** 29-40.

SMITH, J.V. (1953) : Reexamination of the crystal structure of melilite. *Amer. Mineral.,* **38,** 643-661.

SMITH, J.V. & BAILEY, S.W. (1963) : Second review of Al–O and Si–O tetrahedral distances. *Acta Crystallogr.*, **16,** 801-811.

———— (1965) : X-ray-emission microanalysis of rock-forming minerals. I. Experimental techniques. *Journ. Geol.*, **73,** 830-864.

WARREN, B.E. (1930) : The structure of melilite, $(Ca,Na)_2(Mg,Al)(Si,Al)_2O_7$. *Z. Kristallogr.*, **74,** 131-138.

Manuscript received September, 1969, emended December 1969.